Near-surface modeling and statics challenges

Karen Richard* and James Leberknight, SIGMA³ Integrated Reservoir Solutions

This paper was prepared for presentation during the 13th International Congress of the Brazilian Geophysical Society held in Rio de Janeiro, Brazil, August 26-29, 2013.

Abstract

Near-surface modeling is a critical and interpretative step early in the seismic data processing flow. It is interpretative from first break picking to the construction of a geologically feasible model because several approaches may be required to yield the optimal statics solution. This paper will show several of the options available for the critical decisions that must be made during this process. Whether derived from the conventional refractor velocity and delay time method or tomography, these near-surface statics are vital for the accuracy of the data processing flows that follow, preventing incorrect and possibly costly interpretations.

Introduction

The quality of the first break picks is vital to the creation of the near-surface model and statics calculation. First arrivals in the shot records can consist of direct arrivals for the nearest offsets, refracted arrivals, and possibly even reflected arrivals at the farthest offsets in some cases. The basic refraction equation is as follows:

$$T_{AB} = T_A + D_{AB} / V_R + T_B \qquad (1)$$

where

T_{AB} is the first arrival time from the source at A to the receiver at B

T_A is the delay time of the source at A

D_{AB} is the distance from A to B

V_R is the velocity of the refracting layer

T_B is the delay time of the receiver at B

For tomography, we are interested in the nearest offsets as well as the refracted arrivals for the optimal creation of the near-surface velocity model. This method calculates raypath segments through a 3-dimensional grid of nodes, estimating the velocity between each node. This is an iterative process, where travel times through the initial model are compared with the recorded times and then the model is updated from the differences in time.

Data Example 1: Polo Ranch 3D in Southeastern Wyoming

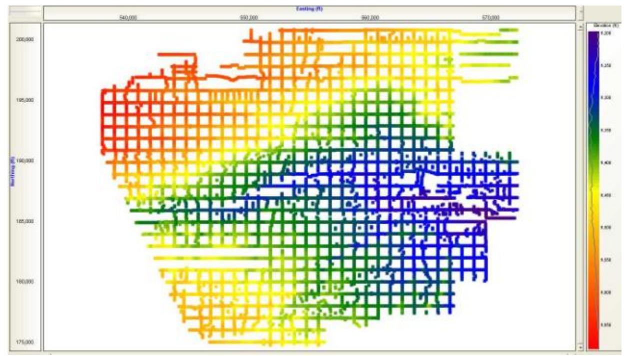

Figure 1: Surface elevations: 6200 (purple)-6650 ft (red)

This was a Vibroseis survey. After a reasonable range of first breaks was determined and picked (blue points below), a refractor was defined consistently at several locations throughout the survey based on the consistency of its velocity when linear move-out (LMO) was applied to the picks and/or traces. We have found in general that a single, well-defined refractor provides as good, if not better, statics solutions than multiple refractors do. This offset range is indicated by the shaded traces in Figure 2 for one such location.

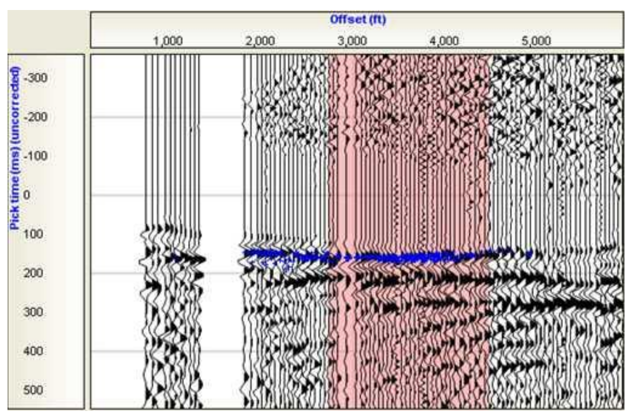

Figure 2: Refractor Definition--shaded traces represent a refractor offset range with LMO applied

Once pick quality was confirmed, refractor velocity and delay time analyses were performed and geometry corrections were calculated from any residual times that remained in the solution. Next, a weathering velocity scan was performed with a range of velocities. When the refractor elevations showed independence from the surface elevations (neither paralleling nor mirroring the surface), the velocity value that was chosen as the desired initial weathering velocity was 4000 ft/s. (Figure 3)

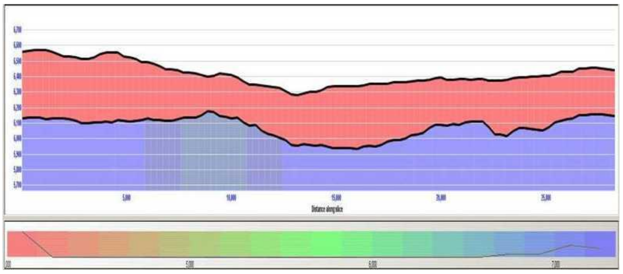

Figure 3: Initial weathering layer velocity = 4000 ft/s (pink) prior to smoothing the refractor. The velocity of the refracting layer below varies from 6500 to 7000 ft/s

After applying a spatial smoother to the refractor elevations, which in effect transfers the high frequency variations from the refractor elevations to the weathering velocities, statics were calculated using a final datum and replacement velocity.

$$\text{Static} = -T\_R - T\_RF \qquad (2)$$

where T_R is the travel time from the source or detector to the top of the deepest refractor using the velocities of each layer, and T_RF is the travel time from the top of the deepest refractor to the final datum, using the replacement velocity.

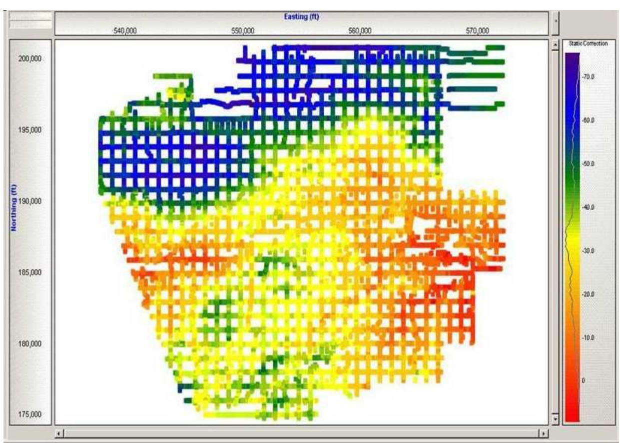

Figure 4: Source and receiver refraction statics: -70ms (purple) to +10ms (red)

Comparison stacks before and after refraction statics application appear in Figures 5 and 6 and show significant improvement at this early stage of processing.

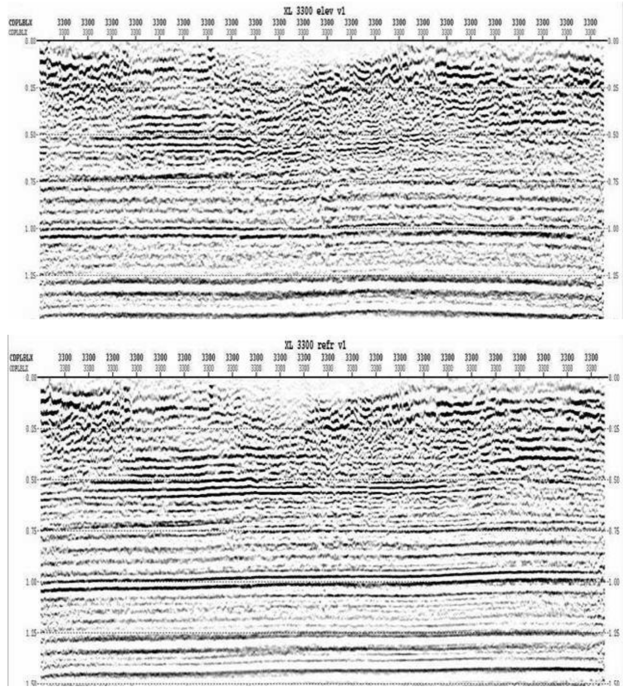

Figure 5: S-N line before (above) and after (below) refraction statics application

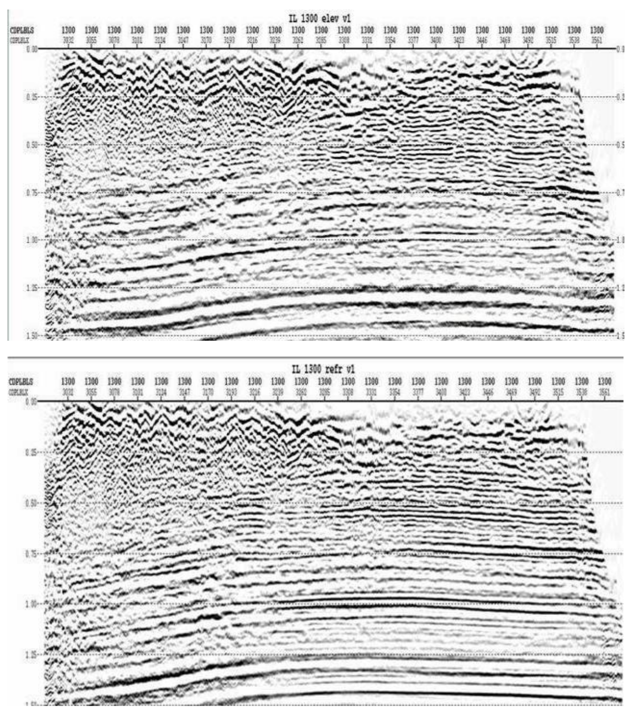

Figure 6: W-E line before (above) and after (below) refraction statics application

Data Example 2: Hainesville Dome 3D in Eastern Texas

This 3D survey was obtained primarily with dynamite sources and about 10% Vibroseis sources.

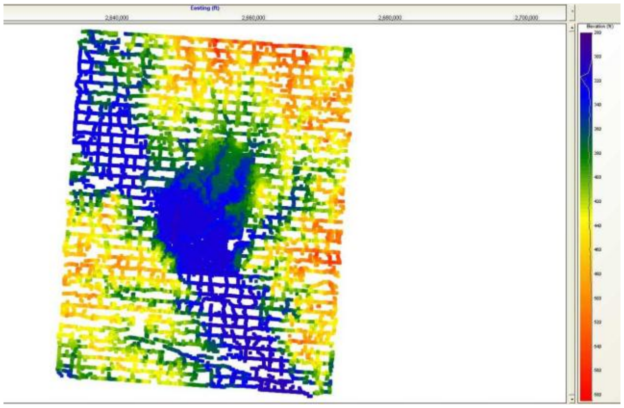

Figure 7: Surface elevations: 280 (purple) to 580 ft (red)

This survey is named for the Hainesville Salt Dome, and its presence can be seen affecting the surface elevations in the center of the survey.

After phase-matching the two source types, first breaks were picked and edited for traces with offsets of 0 to 7000 ft. Source and receiver position errors were verified and corrected, and refractor velocity and delay time analyses were run for a refractor with offsets that averaged from 2000 to 3500 ft. This survey presented an additional challenge, as picks needed to be edited that were affected by the faster velocity of the salt dome to prevent contamination of the statics solutions. We have found that this practice provides superior results when dealing with salt domes. There was still enough pick redundancy remaining at these offsets and receiver locations to produce stable solutions, since source and receiver density was increased over the dome.

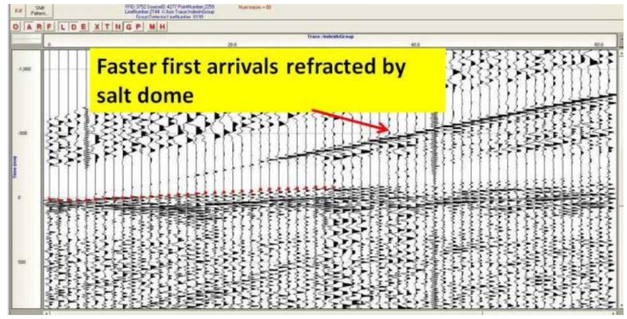

Figure 8: First breaks showing effect of salt dome velocity

Two cross sections of the model that intersect above the salt dome are shown in Figure 9.

Figure 9: Model cross sections after the refractor has been smoothed. V_W varies from 2500 to 3500 ft/s and V_R varies from 6500 to 7100 ft/s

The conventional delay time statics solution improved the stack response, as displayed in Figure 10.

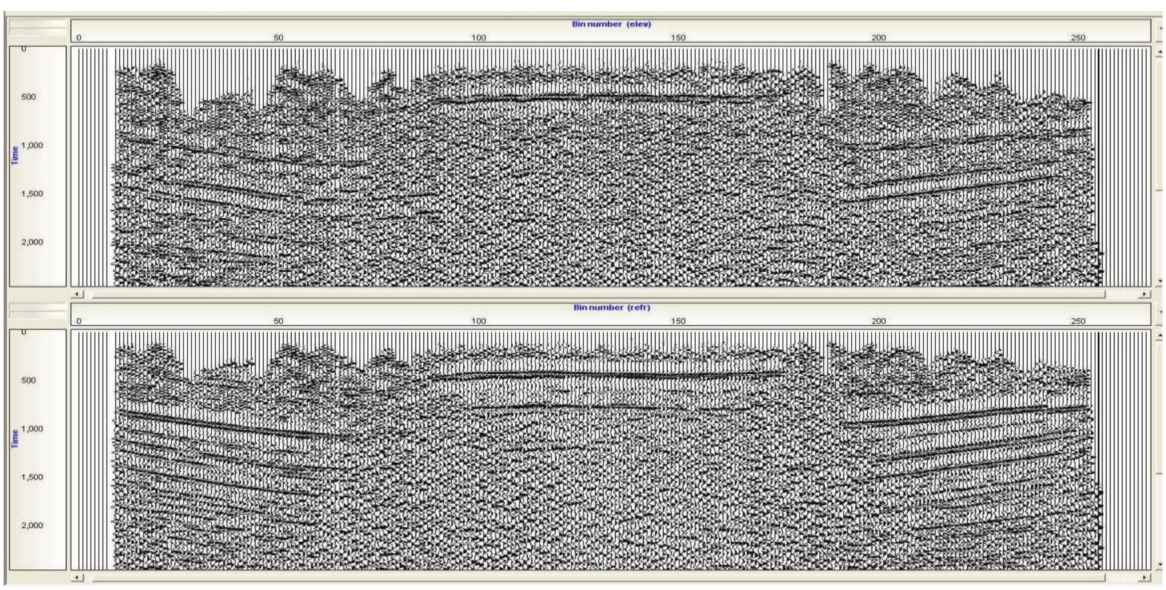

Figure 10: Stack with elevation statics (above) and with refraction statics (below)

Several iterations of tomography were also run on this survey, and the resulting velocity model is shown in Figure 11.

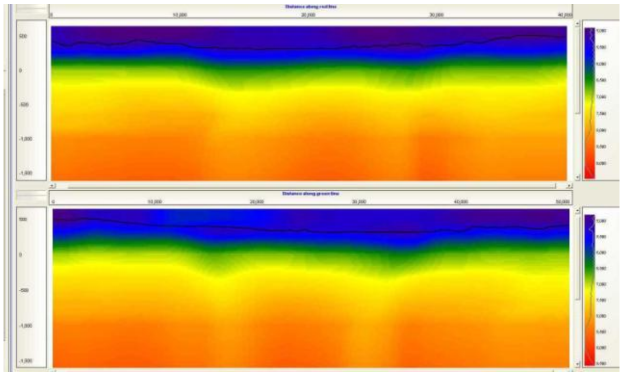

Figure 11: Cross sections of the tomographic velocity model, ranging from 5500 to 8000 ft/s

Tomography can provide a superior solution for the long wavelength statics. We generally run it to provide an alternate statics solution when it is feasible to do so. Tomography is the preferred method in cases where it is very difficult to define distinct refractors because the velocity field is more of a gradient or where velocity inversions are present. We have also developed a tomo-hybrid method, in which we add back the higher frequency residual statics that remain after the long wavelength statics are addressed. Although the three statics solutions were comparable for this survey, the conventional delay time solution was preferred.

In addition, an anisotropic velocity analysis was performed. Figure 12 illustrates the magnitude of the anisotropy that is present, which is the percent difference between the fastest and slowest velocities. A delay time analysis can then be performed with this velocity field and an anisotropic statics solution can be calculated.

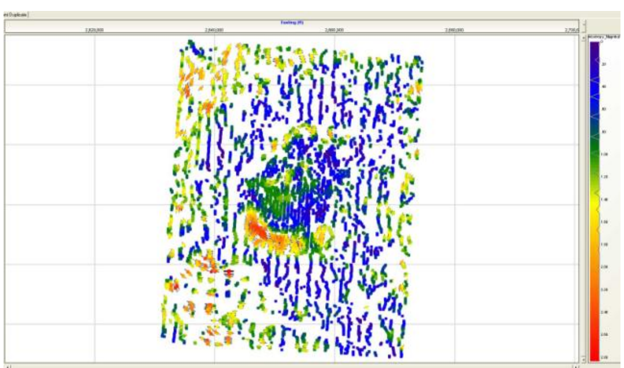

Figure 12: Magnitude of anisotropy varies from 0% (purple) to 2.8% (red)

Data Example 3: 3D in North Central Oklahoma

This survey was primarily Vibroseis with approximately 10% dynamite sources and had more variability in the surface topography, including a river channel (Figure 13).

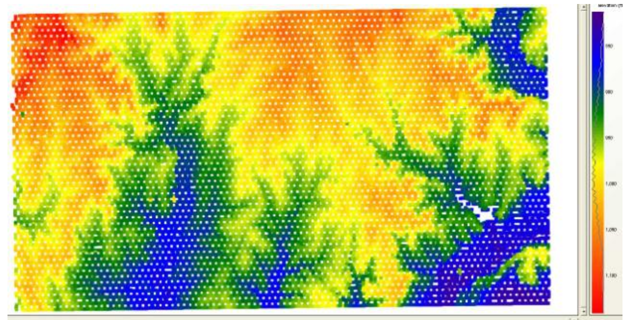

Figure 13: Surface elevations: 800 ft (purple) to1150 ft (red)

After phase-matching the two source types, first breaks were picked for a wide range of offsets. Time constraints did not permit the cleaning up of picks for more than one refractor, which is shown in Figure 14. In this display, refractor offset extent is defined by changes in velocity of the first break picks.

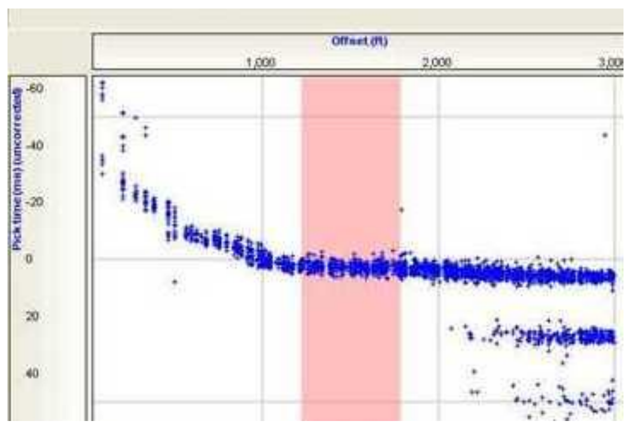

Figure 14: Refractor definition (picks with LMO applied)

Refractor velocity and delay time analyses were run and geometry errors were corrected. Several weathering velocities were tested, and 7000 ft/s was selected. Figure 15 shows the smoothed refractor model through a cross section of the survey. The river channel on the east (right) side of the survey affects both the surface topography as well as the refractor depth (Figure 16).

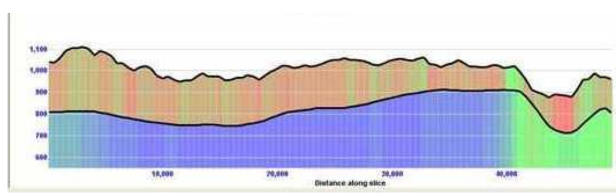

Figure 15: Cross-section of model after smoothing the refractor: 5000 ft/s (pink) to 13000 ft/s (blue)

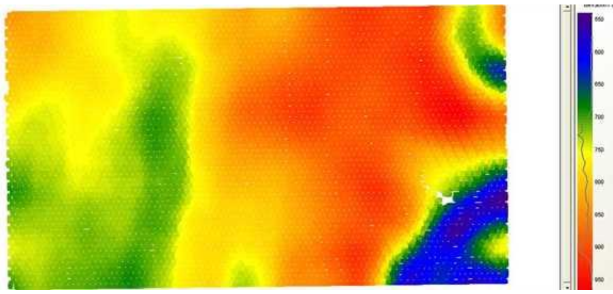

Figure 16: Refractor elevations: 550 ft (purple) to 950 ft (red)

The refraction statics were computed using an intermediate datum that was shifted down 50 feet from the refractor with an additional smoother applied to it.

Using an optional intermediate datum incorporates the refractor velocity in the statics calculation:

$$\text{Static} = -T\_R - T\_RI - T\_IF \qquad (3)$$

where

T_R is the travel time from source or detector to the top of the deepest refractor, using the velocities of each layer;

T_RI is the travel time from the top of the deepest refractor to the intermediate datum, using the velocity of the deepest refractor;

T_IF is the travel time from the intermediate datum to the final datum, using the replacement velocity.

Figure 17 is a display of the final source and receiver refraction statics for this survey.

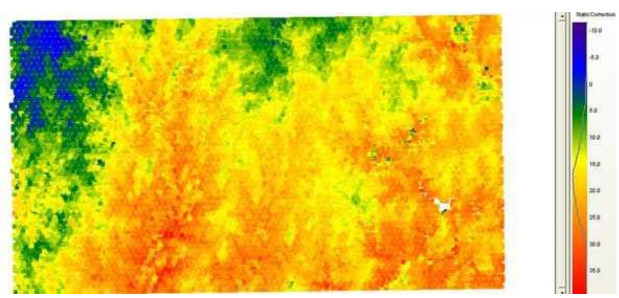

Figure 17: Refraction statics: -10 ms (purple) to 35 ms (red)

Figure 18 is a stack comparison that shows the significant improvement that the refraction statics have made in the first 1000 ms of data, particularly on the right where the river channel is located.

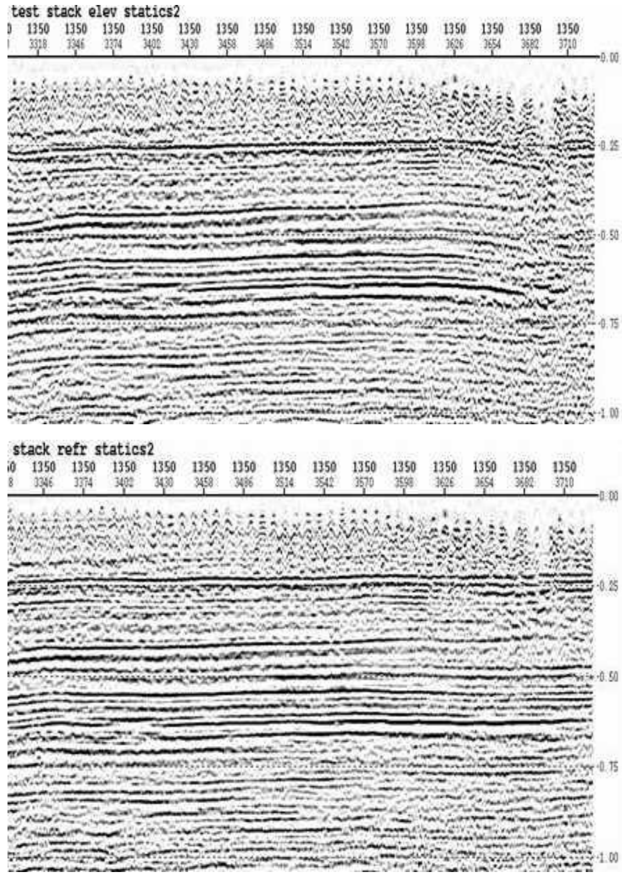

Figure 18: W-E stacks before (above) and after (below) refraction statics application

Conclusions

Near surface modeling is an integral step in data processing. There are several interpretative steps involved as well as several methods available to arrive at the optimal solution for near surface statics issues. Whether conventional delay time, tomography, tomo-hybrid or anisotropic statics are used, the improvement from this one stage early in the processing sequence can be dramatic.

Acknowledgements

I would like to thank DJ Resources, Energy Production Corporation and New Gulf Resources for providing permission to use their surveys in this presentation. I would also like to thank Walter Kessinger of SIGMA^3 for his guidance in the preparation of this paper and Todd Hibbitts, also of SIGMA^3, for the geometry preprocessing of the Hainesville Dome 3D.